Desalination and Water Treatment
www.deswater.com
doi: 10.5004/dwt.2022.28361

256 (2022) 235–241
April

Effect of support columns under deflector on vortex settling basin performance

Lin Li[a,b], Zhuoyun Mu[a,b], Yiyi Ma[c,*]

[a]*College of Water Conservancy and Civil Engineering, Xinjiang Agricultural University, Urumqi 830052, China, emails: lilin_xjau@163.com (L. Li), 7237855mu@sina.com (Z. Mu)*
[b]*Xinjiang Key Laboratory of Hydraulic Engineering Security and Water Disasters Prevention, Urumqi 830052, China*
[c]*College of Civil Engineering and Architecture, Zhejiang University, Hangzhou 310058, China, emails: yiyima@zju.edu.cn (Y. Ma) https://orcid.org/0000-0003-3874-0306*

Received 31 August 2021; Accepted 1 March 2022

ABSTRACT

To avoid the failure of a vortex settling basin (VSB) caused by excessive sediment deposition on its deflector, support columns have been added under the deflector in engineering practice. In this study, experiments were conducted for VSBs with support columns positioned in three different ways. The parameters measuring the performance of the columned VSBs, including sediment removal efficiency, amount of sediment deposition, water abstraction ratio, sediment flushing efficiency and air core size, were obtained in the experiments and compared with the original VSB without any columns. The experimental results showed that compared to the original VSB, the forced vortex and free vortex formed in all the columned VSBs were weakened and the sediment removal efficiencies were reduced slightly as a consequence. The amount of sediment depositing on the basin floor and the water abstraction ratios of the three columned VSBs were similar to the original VSB at the design flow rate, while larger than the original VSB at a smaller flow rate. Additionally, the sediment removal efficiencies were similar among the columned VSBs, indicating limited effects of the positions of the support columns on removing sediment.

Keywords: Deflector; Sediment removal; Support column; Vortex settling basin; Water abstraction ratio

1. Introduction

The vortex settling basin (VSB) is a secondary sediment treatment facility commonly utilized in hydraulic engineering, which removes sediment from water by forming vortex flow [1–3]. A VSB mainly consists of an inlet canal, a settling basin with a bottom flushing orifice and an outlet canal [4]. The sediment-carrying flow enters the VSB tangentially through the inlet canal and vortex flow is formed in the basin. Water and sediment are separated in the basin with part of the sediment being discharged from the bottom flushing orifice while much of the rest deposits on the basin floor and deflector. Relatively sediment-free water then flows out of the VSB though the outlet canal.

Extensive experiments and numerical studies have been conducted to reveal the features of sediment removal in VSBs. Chapokpour et al. [5] measured the flow field inside a VSB by an acoustic-doppler velocimeter (ADV) and found that the tangential velocity played an important role in the secondary flow characteristics. Chapokpour et al. [6] and Huang et al. [7] simulated the formation of the air core in the VSB basin by using FLOW-3D, and reported that the features of the air core had an effect on the sediment removal of the VSB. Additionally, various retrofits have

* Corresponding author.

been tested to improve VSBs regarding sediment removal, water abstraction ratio, sediment deposition, etc. Amin et al. [8] retrofitted a VSB by installing curvature submerge vanes on the basin floor, which led to a higher sediment removal efficiency and a lower water abstraction ratio of the VSB. Kiringu and Basson [9] optimized the design parameters for VSBs based on the simulations by CFD models.

The deflector, a horizontal torus vane covering half the basin circumference of the VSB, has been constructed widely to regulate the inflow and enhance the vortex strength inside the VSB [10]. Normally, the deflector is reinforced by cables, as shown in Fig. 1a. However, a few VSB failure cases have been reported in China, which were caused by excessive sediment deposition on the deflector, for example, the VSBs at Shanxi Jinghui Canal and Xinjiang Kashgar I Power Station. To prevent such VSB failures, constructing a row of support columns under the deflector has been implemented in engineering practice (Fig. 1b). Nevertheless, there is a concern weather the support columns affect the flow pattern in the basin, and weaken the performance of the VSB as a result. Thus, it is important to figure out the effects of support columns, as well as how they are positioned, on the VSB performance before them being widely implemented. However, there has been few studies on this topic, and no relevant design guideline is available currently.

In this paper, an experimental study was conducted to investigate the performance of three VSBs with support columns positioned in three different ways. The parameters measuring the VSB performance, including sediment removal efficiency, sediment flushing efficiency, water abstraction ratio, mass of sediment deposition and air core sizes were obtained from the experiments. The performances of the columned VSBs were then compared to the original VSB without any support columns. Also, the difference among the three columned VSBs was discussed and the effect of the positions of the columns was presented.

2. Experiments

The VSB model utilized in the experiments was scaled from the prototype VSB in Kashgar, China, following the Froude similarity, as shown in Fig. 2a. The scaling factors for length and velocity were $\lambda_L = L_P/L_m = 60$, $\lambda_V = L_P/L_m = 7.75$ (subscripts P and m for prototype and model, respectively). The physical model was made of 6-mm-thick stainless steel, with a roughness coefficient of 0.007–0.008. It had a rectangular inlet canal of 200 mm × 50 mm × 800 mm (width × height × length). The basin had a diameter of 1,000 mm and a bottom slope of 1:5. The bottom flushing orifice of the basin was 18 mm in diameter. The deflector of the VSB was 200 mm in width and placed 80 mm above the inlet canal.

The experimental setup was designed as a self-circulation system, as shown in Fig. 2b. Four inflow discharges of Q_w = 0.85, 1.05, 1.40, and 1.70 L/s were tested in the experiments. The flow rate was controlled by a valve in the pipeline, labelled as 4 in Fig. 2b. The sediment utilized in the experiments had a specific weight of 2,650 kg/m^3. The gradation size distribution of the sediment particles is shown in Fig. 3, of which D_{50} = 0.02 mm. Before the experiments, the sediment was first added into an upstream mixing tank (labelled as 1 in Fig. 2b), which had a volume of 10 m^3, and well mixed with water by a mixer. The sediment-water mixture was then pumped to a constant-head water supply tank and transported to the inlet canal of the VSB, where the sediment-carrying water was well mixed and a steady sediment concentration of 8.0 kg/m^3 was maintained. The sediment concentration in the experiments was determined based on that in the inlet of the prototype VSB, which varied from 0.37 to 11.0 kg/m^3. When the sediment discharge difference between the inlet and outlet of the VSB was smaller than 1%, it was considered to have reached the equilibrium of sediment transport, and then the experiment was started. Note that the design inflow discharges of the prototype VSB was Q_p = 46.2 m^3/s, and correspondingly, that of the VSB model was Q_m = 1.70 L/s.

In the experiments, each test was run for 2 h. During the experiment, the sediment-water mixture was sampled at the inlet, overflow canal, and bottom flushing orifice with an Erlenmeyer flask (250 mL) every 30 min. The Mettler Toledo electronic balance with an accuracy of 0.001 g was used to measure the mass of the filled Erlenmeyer flask. The sampling was repeated three times and the average weight of the filled Erlenmeyer flask was adopted for the subsequent

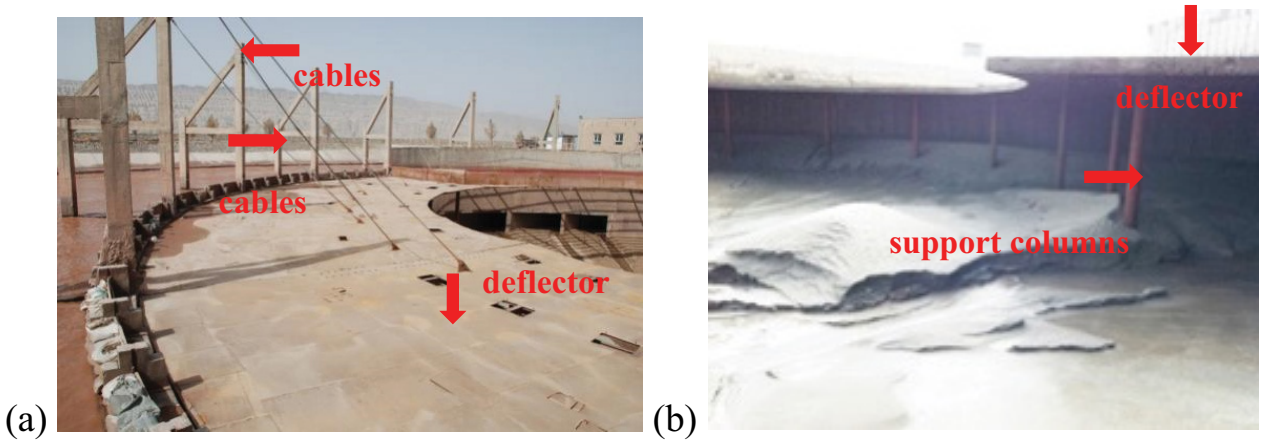

Fig. 1. VSB reinforced with (a) cables and (b) support columns.

(a)

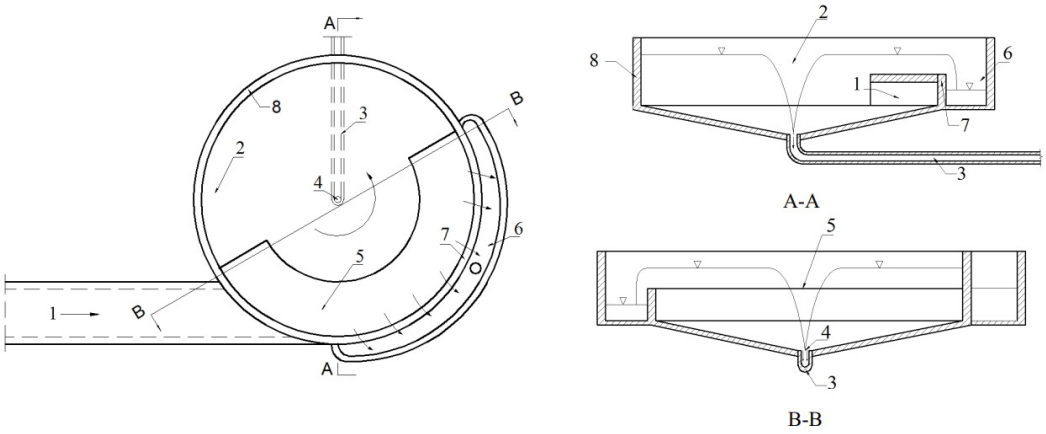

1-inlet canal, 2-VSB basin, 3-flushing pipe, 4-bottom flushing orifice, 5-deflector，
6- overflow channel, 7-overflow weir, 8-basin periphery wall

(b)

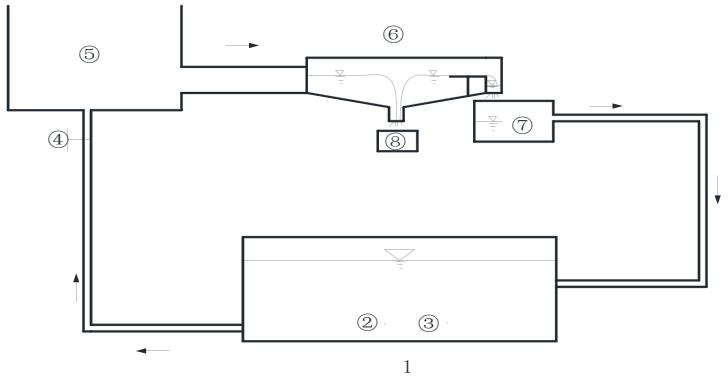

1-mixing tank, 2- pump, 3-mixer, 4-inlet valve, 5-water tank，6-vortex settling basin,
7-measuring weir, 8-collecting tank

Fig. 2. (a) Top and sectional views of the VSB model used in the experiments and (b) schematic of the experimental setup.

analysis. The sediment concentrations in the flow at inlet, outlet canal and the bottom flushing orifice (denoted as S_i, S_o and S_b, respectively) were then obtained by the Displacement Method [11]:

$$S = \frac{(\rho_m - \rho)\times\rho_s}{\rho_s - \rho} = \frac{\left(\frac{M}{V} - \rho\right)\times\rho_s}{\rho_s - \rho} = \frac{\left(\frac{M_m - M_b}{V} - \rho\right)}{\rho_s - \rho} \quad (1)$$

where ρ, M and V are the specific weight, the volume and mass of the calibrated Erlenmeyer flask, respectively. The subscripts of s, m and b are for sediment, sediment-water mixture and bottle, respectively. The inflow discharge (Q_i), water flow rates at the bottom flushing orifice (Q_b) and the outflow canal (Q_o) were measured with the pre-calibrated sharp-crested rectangular weirs. The parameters measuring the VSB performance, that is, the water abstraction ratio λ, the sediment removal efficiency η, and the sediment flushing efficiency μ, were defined as Eqs. (2)–(4):

$$\lambda = \frac{Q_b}{Q_i}\times 100\% \quad (2)$$

$$\eta = \left(1 - \frac{Q_o S_o}{Q_i S_i}\right)\times 100\% \quad (3)$$

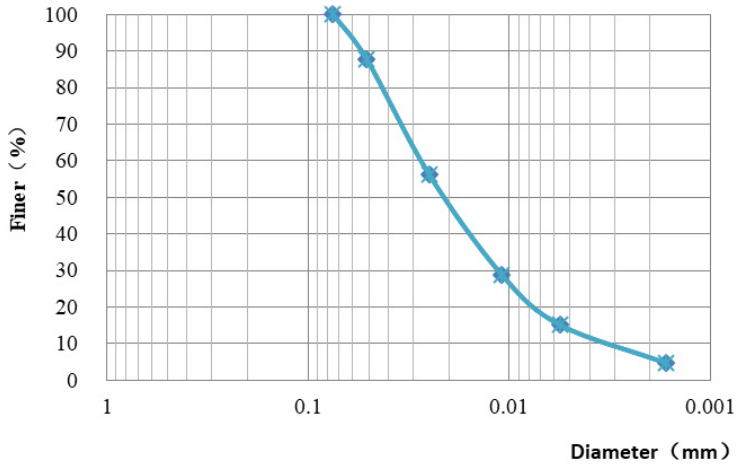

Fig. 3. Grain size distribution of the sediment used in the experiments.

$$\mu = \frac{Q_b S_b}{Q_i S_i} \times 100\% \tag{4}$$

After each test, the sediment depositing on the deflector and the basin floor was collected, dried and weighed.

The 10 columns to support the deflector of the VSB in the experiments had a diameter of 8 mm, and were arranged following the radian of the deflector with an interval radius angle of 17°, as shown in Fig. 4. The support columns were installed in a row located 0.5B, 0.75B and 0.98B away from the basin wall (with B being the width of the deflector), denoted as C_1, C_2, C_3, respectively. Note that the original VSB without any columns under the deflector was donated as C_0 in the current study.

3. Results and discussions

3.1. Assessment parameters

To assess the effects of the support columns, the parameters D_1, D_2, D_3 and D_4 are introduced as the index measuring the change in performance of the columned VSBs compared to the original one, regarding the mass of sediment deposition on the basin floor, the sediment removal efficiency, water abstraction ratio and sediment flushing efficiency, respectively. The assessment parameters are defined as follows:

$$D_1 = \frac{m_i - m_0}{m_0} \times 100\% \tag{5}$$

$$D_2 = \eta_i - \eta_0 \tag{6}$$

$$D_3 = \lambda_i - \lambda_0 \tag{7}$$

$$D_4 = \mu_i - \mu_0 \tag{8}$$

where m in Eq. (5) is the mass of sediment depositing on the basin floor. Here, the parameters with the subscript 0 are for the original VSB C_0 while those with the subscript i are for the columned VSBs C_i (i = 1, 2, 3).

3.2. Experimental observations

The appearances of the VSBs with and without the support columns during the experiments when Q_w = 1.70 L/s are shown in Fig. 5. A demarcation line can be observed, within which the sediment concentration in water is significantly lower than the outside. In essential, the demarcation line is related to the forced vortex formed near the basin periphery and the free vortex in the central region. The relatively clean water area within the demarcation line corresponds to the free vortex region, where the vortex flow velocity is greater and sediment can be separated from water. Much sediment is flushed out of the VSB through the bottom orifice, so the sediment concentration in this area is lowered. In the forced vortex region, the reduction in the vortex strength leads to less significant sediment separation and thus, a more turbid area. The locations of the demarcation line in the four VSBs are expressed as r_m/R_m, with r_m being the radius of the relatively clean water area in the center and R_m the basin radius, as listed in Table 1. The values of r_m/R_m for the VSBs are sorted as $C_0 > C_2 > C_3 > C_1$ under all the working conditions. A larger clear water area indicates a greater free vortex flow velocity. After entering the VSB, the inflow moves along the basin circumference below the deflector under the effect of inertia and the vertical downward restriction of the deflector. The columns can cause head loss for the flow and thus, weaken the free vortex correspondingly. When positioned in the center of the deflector, the columns can cause much resistance to the flow. Therefore, the forced vortex and free vortex velocity of C_1 is smaller than those of C_2 and C_3, leading to a smaller relatively clean water area. The air core sizes in the three columned VSBs are shown in Table 2. It can be found that the air core size of C_0 is the largest. Specifically, when the inflow discharge was smaller than the design flow rate, that is, $Q_w \leq 1.7$ L/s, the air core sizes in the four VSBs are sorted as $C_0 > C_2 > C_3 > C_1$, consistent with that of r_m/R_m. As the air core size is positively correlated with the free

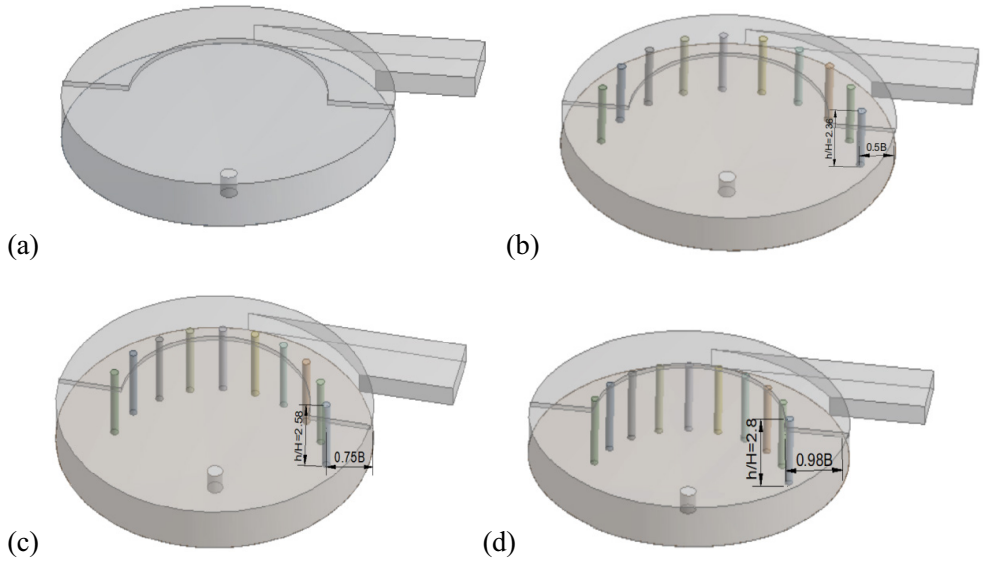

Fig. 4. Different VSBs with the columns installed at different positions: (a) C_0, (b) C_1, (c) C_2 and (d) C_3.

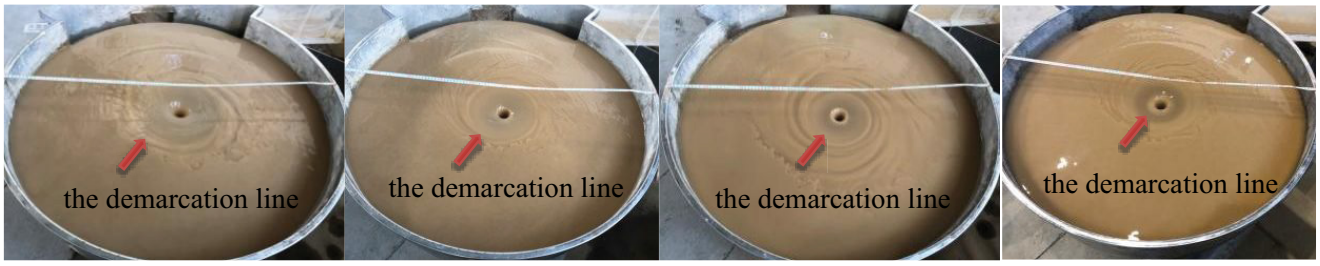

Fig. 5. Flow appearance in different columned VSBs when Q_w = 1.70 L/s: (a) C_0, (b) C_1, (c) C_2 and (d) C_3.

vortex velocity, the results also show that the vortex flow velocity is weakened most significantly when the columns were installed at 0.5B.

3.3. Assessment parameters of columned VSBs

A comparison diagram of the sediment deposition on the basin floor under different experimental conditions is shown in Fig. 6a. D_1, the measure of the difference of sediment deposition between the columned VSBs and the original, are larger than 0 for C_1, C_2 and C_3, indicating a larger sediment deposition of the columned VSBs than the original. Among all the columned VSBs, the amount of sediment deposition on the basin floor of C_2 is the smallest while C_1 the largest. For example, when Q_w = 0.85 L/s, compared with C_0, the amount of sediment deposition on the basin floor of C_1, C_2, and C_3 are increased by 13.44%, 8.79%, and 11.1%, respectively. Considering the smallest air core size in C_1, the strength of forced vortex and free vortex are both the weakest in C_1. When the flow velocity in the basin is less than the sediment-moving incipient velocity, the sediment deposits, of which the amount increases when the water flow velocity decreases. The air core sizes of C_2 and C_3 are close to C_0, both larger than C_1, which indicates little effect of the columns on the vortex strength when positioned at 0.75B and 0.98B. Correspondingly, the flow velocities over the basin bottom in C_2 and C_3 are greater than C_1, resulting in a smaller amount of sediment deposition on the basin floor.

The difference of sediment removal efficiencies of the columned VSBs compared to the original VSB are shown in Fig. 6b. From the results, the variation of sediment removal efficiency is insignificant, with the maximum value no larger than 1%. Thus, the support columns have little effect on sediment removal efficiency of the VSB. Also, where the columns are located does not change the sediment removal efficiency much.

D_3 for measuring the difference of water abstraction ratios are shown in Fig. 6c. D_3 is greater than 0 for all the columned VSBs, indicating an increase in the water abstraction ratio after installing the columns. Among all the columned VSBs, C_2 exhibits the minimum value of D_3 while C_1 the maximum. It is understood that the water abstraction ratio of VSB

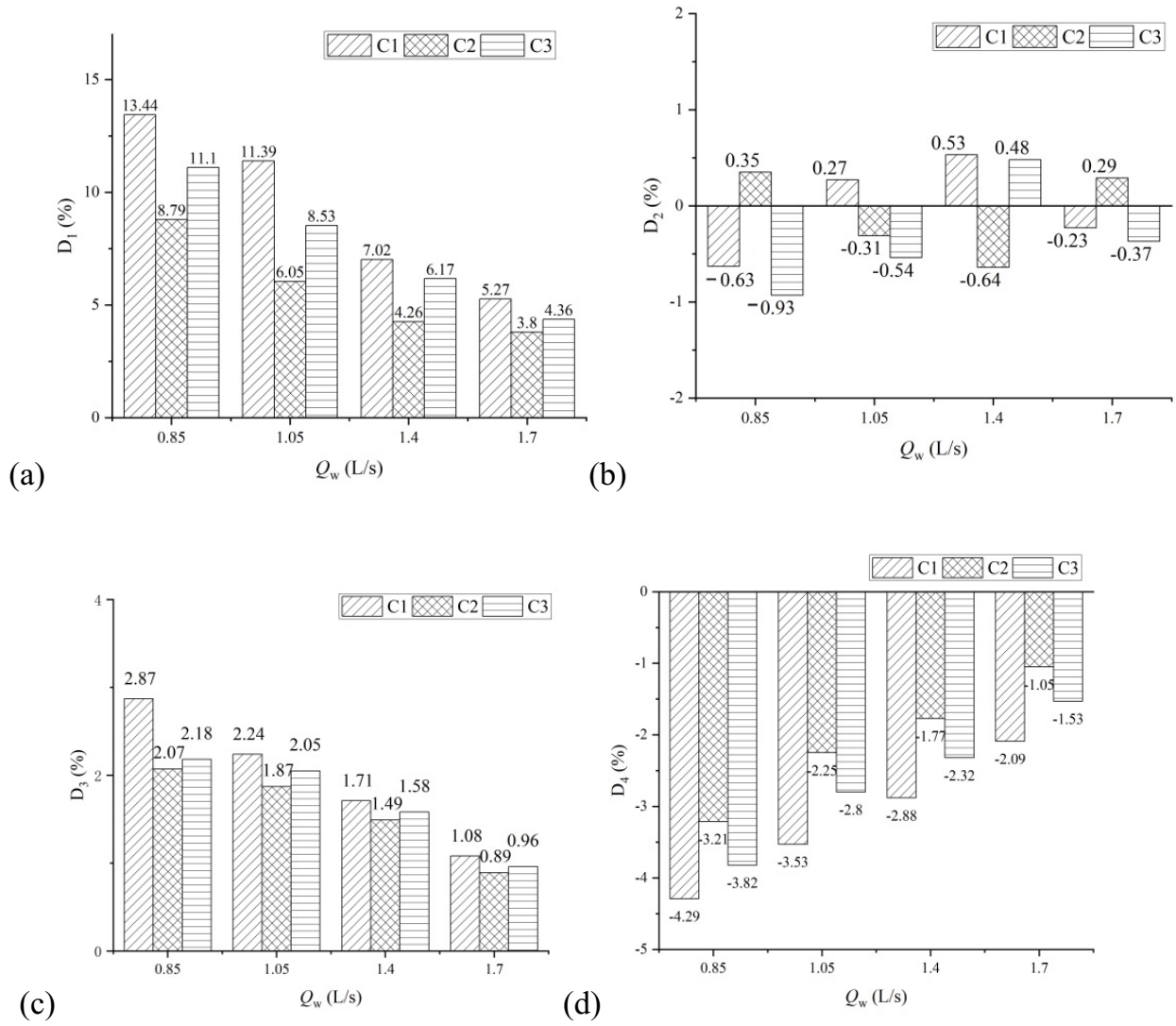

Fig. 6. The performance measuring parameters of the columned VSBs: (a) D_1, (b) D_2, (c) D_3 and (d) D_4.

Table 1
Positions of demarcation line in different VSBs

r_m/R_m / Q_w (L/s)	C_0	C_1	C_2	C_3
0.85	0.23	0.168	0.184	0.172
1.05	0.27	0.21	0.232	0.218
1.40	0.30	0.238	0.268	0.248
1.70	0.32	0.28	0.30	0.286

Table 2
Air core sizes of the three columned VSBs

d / Q_w (L/s)	C_0	C_1	C_2	C_3
0.85	$2.67D_f$	$2.37D_f$	$2.49D_f$	$2.47D_f$
1.05	$2.78D_f$	$2.52D_f$	$2.62D_f$	$2.58D_f$
1.40	$2.83D_f$	$2.62D_f$	$2.69D_f$	$2.65D_f$
1.70	$2.94D_f$	$2.76D_f$	$2.83D_f$	$2.8D_f$

is inversely proportional to the air core size and the vortex velocity. At the same inflow discharge, the air core size of C_1 is the smallest and the vortex strength is the weakest, which results in the largest water abstraction ratio. Additionally, the results show that D_3 decreases with the increase of inflow discharge. It is because that a smaller inflow discharge corresponds to a smaller vortex flow velocity, which leads to a larger water abstraction ratio.

The values of D_4 for measuring the variation of sediment flushing efficiencies are shown in Fig. 6d. All the columned VSBs exhibit negative values of D_4, indicating a reduced sediment flushing efficiency compared with C_0. It is because that head loss occurs when the sediment-carrying water bypassing the columns, which reducing the sediment transport capacity of flow. As a consequence, sediment settled on the basin floor before reaching the central spiral flow

area, which reduced the sediment flushing efficiency. Under all the working conditions, the sediment flushing efficiencies among the columned VSBs are $C_2 > C_3 > C_1$. For example, at Q_w = 0.85 L/s, compared to C_0, the sediment flushing efficiency is reduced by 4.29%, 3.21%, 3.82% for C_1, C_2, and C_3, respectively. The sediment flushing efficiency increases with the increase of the secondary flow velocity at the basin bottom. The vortex in C_2 and C_3 are stronger than that in C_1, resulting in a larger secondary flow velocity over the basin bottom, and thus, the sediment flushing efficiencies of C_2 and C_3 are higher than C_1. In addition, based on the experimental results, the sediment flushing efficiency and water abstraction ratio do not show positive correlation with each other. For example, C_1 has the largest water abstraction ratio while the sediment removal efficiency is the smallest.

According to the experimental results, sediment removal efficiency is basically the same among the three columned VSBs. All the assessment parameters of C_2 are closer to those of the original VSB compared with C_1 and C_3 when the inflow discharge is smaller than the design flow rate. However, the performances of the three columned VSBs are similar when the inflow discharge reaches the design flow rate. Therefore, with the same amount of support columns, the position of the columns has a limited effect on the VSB performance at the design flow rate. Note that in engineering practice, when the inflow discharge does not exceed the design flow rate, the amount of sediment carried by water flow is not significant, which is less likely to cause problems to the VSB. Thus, the positions of the columns can be determined as long as fulfilling the requirement of structural stability.

4. Conclusions

The current study investigated the effect of support columns as well as their positions on the VSB performance. The following conclusions can be obtained:

- The installation of support columns under the deflector reduced the forced vortex flow velocity in the basin and the induced free vortex flow velocity.
- A demarcation line for turbid and relatively sediment-free area was observed in the experiments. When the columns were installed at 0.5B, the relatively clear water area in the VSB is the smallest and the free vortex flow velocity in the basin is the smallest.
- The air core sizes of the columned VSBs were smaller than that in the original VSB, which resulted from the reduction in the strength of vortex flow caused by the columns.
- At the design flow rate, the amount of sediment deposition on the basin floor and the sediment removal efficiencies of the columned VSBs were similar, all close to the original VSB. The position of the columns had a limited effect on the VSB performance at the design flow rate. Considering the low risk of VSB failures when the flow rate is smaller than the design flow rate in engineering practice, the positions of the columns can be determined as long as fulfilling the requirement of structural stability.

Acknowledgment

The writers gratefully acknowledge financial support from the National Natural Science Foundation of China (Grant No. 52069028), the University Research Project of Xinjiang Uygur Autonomous Region (Grant No. XJEDU2018I010), Tianshan Youth Project (2018Q017), and the Fundamental Research Funds for the Central Universities (2020QNA4017).

Symbols

D_{50}	—	Particle diameter representing the 50% cumulative percentile value
D_i	—	Assessment parameters for VSBs (i = 1, 2, 3, 4)
M	—	Mass
Q	—	Water flow rate
r_m	—	Radius of relatively clean water area in the center of VSB
R_m	—	VSB basin radius
S	—	Sediment concentration
V	—	Volume
η	—	Sediment removal efficiency
λ	—	Water abstraction ratio
μ	—	Sediment flushing efficiency
ρ	—	Specific weight

Subscripts

m	—	Model
p	—	Prototype

References

[1] F.S. Salakhov, Rotational Design and Methods of Hydraulic Calculation of Load-Controlling Water Intake Structures for Mountain Rivers, Proc. of Ninth Congress of the ICID, Moscow Soviet Union, 1975, pp. 151–161.
[2] A.R. Keshavarzi, A.R. Gheisi, Trap efficiency of vortex settling chamber for exclusion of fine suspended sediment particles in irrigation canals, Irrig. Drain., 55 (2006) 419–434.
[3] Q.-T. Nguyen, C.-D. Jan, Sediment Removal Efficiency of a Deep Vortex Chamber Sediment Extractor, Environmental Hydraulics, 2010, pp. 1065–1070.
[4] T.C. Paul, S.K. Sayal, V.S. Sakhuja, G.S. Dhillon, Vortex-settling basin design considerations, J. Hydraul. Eng.-ASCE, 117 (1991) 172–189.
[5] J. Chapokpour, J. Farhoudi, E.A. Tokaldany, M. Majedi-Asl, Flow visualization in vortex chamber, J. Civ. Eng. Urbanism, 2 (2012) 26–34.
[6] J. Chapokpour, F. Ghasemzadeh, J. Farhoudi, The numerical investigation on vortex flow behavior using FLOW-3D, Iran. J. Energy Environ., 3 (2012) 88–96.
[7] T.-H. Huang, C.-D. Jan, Y.-C. Hsu, Numerical simulations of water surface profiles and vortex structure in a vortex settling basin by using flow-3D, J. Mar. Sci. Technol.-Taiwan, 25 (2017) 531–542.
[8] H. Amin, S. Mojtaba, A.M. Mehdi, Effects of curvature submerge vane in efficiency of vortex settling basin, J. Appl. Res. Water Wastewater, 2 (2014) 80–85.
[9] K. Kiringu, G. Basson, Removal of Fine Non-Cohesive Sediment by Swirl/Vortex Settling Basin at Small River Abstraction Works, 19th Int. Conf. on Transport and Sedimentation of Solid Particles, Cape Town, South Africa, 2019, pp. 24–27.
[10] D.A. Mashauri, Modeling of a Vortex Settling Basin for Primary Clarification of Water, Tampere University of Technology, Tampere, Finland, 1986.
[11] T. Qihua, Y. Laifei, Sediment Design Manual. Being, China Water & Power Press, China, 2006 (in Chinese).